

Compatibilization of *i*PP/HDPE Blends with PE-*g*-*i*PP Graft Copolymers

Kristine Klimovica, Sanshui Pan, Ting-Wei Lin, Xiayu Peng, Christopher J. Ellison,* Anne M. LaPointe,* Frank S. Bates,* and Geoffrey W. Coates*



Cite This: *ACS Macro Lett.* 2020, 9, 1161–1166



[Read Online](#)

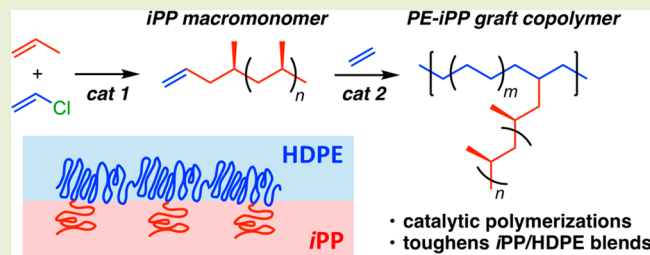
ACCESS |

Metrics & More

Article Recommendations

SI Supporting Information

ABSTRACT: The compatibilization of polyethylene (PE) and isotactic polypropylene (iPP) blends is of particular interest due to the challenges associated with recycling these plastics from mixed waste streams. Polyethylene-*graft*-iPP copolymers (PE-*g*-iPP) were prepared using a grafting-through strategy by copolymerization of ethylene with allyl-terminated iPP macromonomers in the presence of a hafnium pyridylamido catalyst. Graft copolymers with a variety of graft lengths ($M_n = 6-28$ kg/mol), graft numbers, and graft spacings were prepared. These graft copolymers were melt-blended with high-density polyethylene (HDPE) and iPP (iPP/HDPE = 30/70 w/w), and the blend properties were evaluated by tensile testing. The blends showed enhanced tensile strength at 5 and 1 wt % loading, with higher tensile strength observed for larger block numbers and graft lengths. These results indicate that graft copolymers are efficient compatibilizers for blends of HDPE and iPP.



Plastics are an integral part of modern society, and the production of industrial polymers has increased dramatically since 1970.¹ Unfortunately, most plastics are disposed of in landfills or the environment. This is a major concern for polyethylene (PE) and isotactic polypropylene (iPP), which account for 2/3 of all polymers produced worldwide and are commonly employed in single-use applications such as packaging. Currently, approximately 1% of iPP and less than 7% of PE are recycled.² The low recycling rate is largely due to the recycling challenges presented by mixed polyolefin waste streams. High-density polyethylene (HDPE) and iPP are commonly found together in commingled plastic waste and are difficult to separate using optical or density sorting technologies. Melt reprocessing HDPE and iPP waste into a blend product is one potentially useful way to circumvent the need for separation of the waste streams. However, blends of HDPE and iPP are often brittle and have poor mechanical properties due to phase separation of the two polymers.³

The majority of HDPE and iPP produced industrially are made using heterogeneous catalysts. Chaffin et al. showed that HDPE and iPP prepared with heterogeneous catalysts contain significant amounts of noncrystallizable, amorphous material,⁴ which rapidly migrates to the interface and inhibits entanglements, cocrystallization, and adhesion.⁴ Therefore, the ability to overcome the interfacial activity of amorphous chains is very important. The addition of nonreactive compatibilizers to HDPE and iPP blends is one way to improve their mechanical properties and represents a potential pathway for utilization of mixed waste recycling streams.³ Current strategies for nonreactive compatibilization of HDPE

and *i*PP rely on using relatively large amounts (≥ 10 wt %) of amorphous copolymer additives. While portions of these copolymers are usually miscible with HDPE and *i*PP giving rise to some compatibilization activity, the use of such large additive quantities results in plasticization that deteriorates the physical properties of the blend.^{5,6} Block copolymers have found application in compatibilization of other types of polymers⁷⁻⁹ and offer an attractive route for compatibilization of HDPE and *i*PP.

Dow Chemical has reported the use of olefin block copolymers (OBC)¹⁰ as compatibilizers and adhesives.¹¹ The tensile properties of *i*PP–HDPE blends were improved with the addition of 10 wt % of a PE-poly(ethylene-*co*-octene) (PE-EO) OBC, which was attributed to enhanced adhesion between HDPE and *i*PP domains.¹² PE-*i*PP diblock copolymers (sold commercially as INTUNE) were also tested as compatibilizers¹³ and tie layers¹⁴ for PE and *i*PP. As was the case with the PE-EO OBCs, compatibilization of the *i*PP–HDPE blends was observed at relatively high loading levels (5–10 wt %). However, due to the nature of the chain shuttling chemistry used to produce the OBCs, they are comprised of various block lengths and different numbers of

Received: May 4, 2020

Accepted: July 10, 2020

blocks per chain. As part of our ongoing research into precision polymer synthesis and phase separation, we are interested in developing a fundamental understanding of how specific copolymer architectures influence compatibilization efficiency.

We recently reported that the addition of linear polyethylene-*block*-iPP (PE-*b*-iPP) multiblock copolymers to PE and iPP blends significantly improved the tensile properties at low additive loadings (Scheme 1a).¹⁵ The well-defined nature

of the multiblock additive as well as the controlled manner of synthesis allowed a systematic study of the effects of the number and sizes of the blocks on the efficacy of compatibilization.¹⁶ However, this work relies on the use of a living catalyst system that produces one polymer chain per catalyst, increasing the cost and potentially reducing its industrial utility.

In our previous studies on polyolefin-based thermoplastic elastomers, we found that the physical properties of well-defined graft copolymers featuring semicrystalline side chains and amorphous backbones rivaled or exceeded those of linear block copolymers and could be prepared using nonliving polymerizations.¹⁷ The graft copolymer elastomers were prepared using a “grafting through” strategy by copolymerizing allyl-terminated iso- or syndiotactic polypropylene macromonomers with mixtures of ethylene and octene or propylene. We were interested in whether a similar strategy could be applied for the synthesis of compatibilizers.¹⁸ Graft copolymers (GCPs) containing a semicrystalline PE backbone and iPP side chains (PE-*g*-iPP) were previously prepared via a “grafting to” method by the reaction of hydroxyl-terminated iPP with maleated PE.¹⁹ However, the presence of substantial amounts of difunctionalized iPP led to the formation of mixtures of polymer architectures. Recently, Tsou and co-workers reported that comb-block copolymers containing a PE main chain and atactic polypropylene grafts can compatibilize HDPE and iPP.^{20,21} These GCPs showed great reduction in microdomain size and an increase in elastic modulus; these results show that graft architectures can compatibilize polyolefin blends. Based on Tsou’s results and our own experience with PE/iPP compatibilization, we envisioned that PE-*g*-iPP graft copolymers (Scheme 1b) might be suitable compatibilizers and

Scheme 1. Additives for Compatibilization of iPP/HDPE Blends: (a) Well-Defined PE-*b*-iPP Multiblock Copolymers; (b) PE-*g*-iPP Graft Copolymers; (c) PE-*g*-iPP Graft Copolymer Architectural Variations

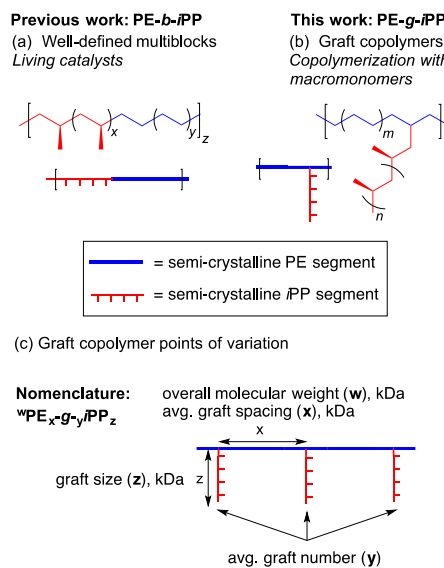


Table 1. Synthesis and Characterization of Graft Copolymers^a

entry	sample ^b	iPP MM ^c (kDa)	mass MM (g)	C ₂ H ₄ (psi)	yield (g)	MM incorp. ^d (%)	graft/chain ^e	ϵ^f (%)
1	¹⁸⁵ PE _{5.2} - <i>g</i> - ₁₆ iPP ₆	6	1.00	10	1.33	40	16	950 ± 50
2	²²¹ PE ₁₅ - <i>g</i> - ₁₀ iPP ₆	6	1.00	20	1.88	45	12	100 ± 60
3 ^g	⁶³ PE _{5.5} - <i>g</i> - _{5.0} iPP ₆	6	1.00	10	1.20	21	5.0	n.d. ^h
4	¹⁶⁴ PE ₁₃ - <i>g</i> - _{5.5} iPP ₁₄	14	0.50	10	0.73	40	5.5	57 ± 16
5	²¹⁰ PE _{8.9} - <i>g</i> - _{8.8} iPP ₁₄	14	0.75	10	1.04	53	8.8	850 ± 30
6	²⁶⁰ PE _{8.8} - <i>g</i> - ₁₁ iPP ₁₄	14	1.00	10	1.46	60	11	990 ± 80
7	²¹³ PE _{5.7} - <i>g</i> - _{2.2} iPP ₁₄	14	1.00	20	1.73	12	2.2	210 ± 20
8 ⁱ	³⁶⁴ PE _{7.4} - <i>g</i> - _{2.9} iPP ₂₆	26	1.00	10	1.99	26	2.9	17 ± 2
9 ⁱ	²⁹⁸ PE ₃₀ - <i>g</i> - _{4.6} iPP ₂₈	28	1.50	10	2.05	29	4.6	31 ± 4
10 ⁱ	³⁹⁸ PE ₁₅ - <i>g</i> - _{9.3} iPP ₂₆	26	2.00	10	2.52	40	9.3	910 ± 80
11 ⁱ	⁴¹³ PE ₃₉ - <i>g</i> - _{5.6} iPP ₂₈	28	2.00	20	3.08	33	5.6	620 ± 180
12 ^{g,i}	³²⁰ PE _{9.8} - <i>g</i> - _{8.2} iPP ₂₈	28	2.00	10	2.36	46	8.2	910 ± 70

^aGeneral conditions: 10.0 μ mol **1**, 10.5 μ mol $B(C_6F_5)_3$, 50 mL of PhMe, 0.50 to 2.00 g of macromonomer (MM), 30 min. ^bGraft copolymer nomenclature: $wPE_x-g_y-iPP_z$, where $w = M_p$ of the polymer, $x = M_n$ of the average PE spacers, $y =$ average iPP grafts per chain, $z = M_n$ of iPP macromonomer (see SI for calculation details). ^cDetermined by GPC relative to polyethylene standards at 150 °C in 1,2,4-trichlorobenzene. ^dCalculated from area of the unreacted MM using area vs GPC sample mass plot (see SI for details). ^eCalculated as moles of macromonomer incorporated divided by the moles of graft copolymer. ^f ϵ = average strain at break and standard deviation (%) for HDPE/iPP 70/30 blends with 5 wt % graft copolymer additive determined at fracture using uniaxial tensile test. Tensile bars were cooled at 10 K/min after melt-pressing (HDPE: $\epsilon = 1180 \pm 170\%$; iPP: $\epsilon = 560 \pm 50\%$; HDPE/PP 70/30: $\epsilon = 17 \pm 1\%$). ^gCopolymerization time = 15 min. ^hn.d. = not determined. ⁱ100 mL of toluene.

permit the use of nonliving polymerizations for both the production of the macromonomer and graft copolymer, resulting in a viable alternative to living polymerization. In addition, *i*PP grafts are advantageous for their potential to cocrystallize with the *i*PP homopolymer, strengthening their ability to transfer stress across PE–*i*PP interfaces. Important variables for GCPs include *i*PP graft length, number of grafts per chain, average distance between grafts, branch distribution, and backbone length (Scheme 1c). The results of this study are reported below.

A series of allyl-terminated *i*PP macromonomers was prepared using an *ansa*-metallocene catalyst that can undergo β -chloride elimination in the presence of a vinyl chloride chain transfer agent.^{22,23} The macromonomers were characterized by gel-permeation chromatography (GPC) and were prepared over a range of molecular weights ($M_n = 6$ –28 kg/mol) by varying the amount of vinyl chloride added (Table S1).

A series of graft copolymers were prepared by copolymerization of the *i*PP macromonomers with ethylene (Table 1) using a Hf pyridylamido precatalyst (1) and $B(C_6F_5)_3$. To ensure macromonomer and graft copolymer solubility, the copolymerizations were run at 70 °C, and the reaction was quenched prior to full macromonomer consumption to help minimize tapering in the resulting graft copolymers. Since the graft copolymers used in the study contained unreacted macromonomer, all measurements were normalized for residual monomer. GPC curve fitting was used to estimate the amount of residual unreacted macromonomer in the mixture and to calculate the average number of grafts incorporated per polymer chain; the amount of macromonomer incorporated ranged from 12–60%. A full description of the residual macromonomer quantification is given in the Supporting Information (Figures S1 and S2 and Table S2). Graft copolymer overall molecular weight (w) is reported as M_p rather than M_n due to the overlap of the GPC trace with that of residual monomer.

The number of grafts incorporated into the chain can be tuned by adjusting the macromonomer concentration in the polymerization (Table 1, entries 4–6 and 8–10). The polyethylene weight fraction can be tuned by varying the ethylene pressure (Table 1, entries 1 vs 2; 6 vs 7; 10 vs 11). To determine if the grafts were randomly distributed along the main polymer chain, control experiments were performed by stopping the polymerization early. The polymer synthesized using this method contained fewer grafts per chain, suggesting that incorporation of the macromonomer is continuous throughout the duration of the experiment (Table 1, entries 1 and 3). However, for the highest molecular weight macromonomers ($M_n = 26$ –28 kDa), we noticed that, at high macromonomer concentration, the number of grafts was unchanged from 15 to 30 min reaction times (Table 1, entries 12 and 10, respectively), although the total molecular weight increased. We hypothesize that the high molecular weight macromonomer has low solubility under reaction conditions and coprecipitates with the growing polymer chains as reaction becomes more saturated with polymer, inhibiting further incorporation.²⁴ Since the majority of the high molecular weight macromonomer incorporation occurs toward the beginning of the polymerization, this may result in graft copolymers with a higher density of grafts located toward one end of the polymer chain. Additional synthetic studies are needed to fully understand the details of this effect.

*i*PP and HDPE homopolymers undergo phase separation when blended in the melt. To investigate the effect of GCPs on blend structure, mixtures of *i*PP and HDPE (*i*PP/HDPE = 30/70 w/w) were melt-blended in the presence of a graft copolymer (5 wt %). The morphology of the mixtures was imaged by transmission electron microscopy (TEM). The blends were stained with a RuO_4 solution²⁵ and then cryomicrotomed. Representative TEM micrographs are shown in Figures 1, S4 and S5, where the *i*PP minority

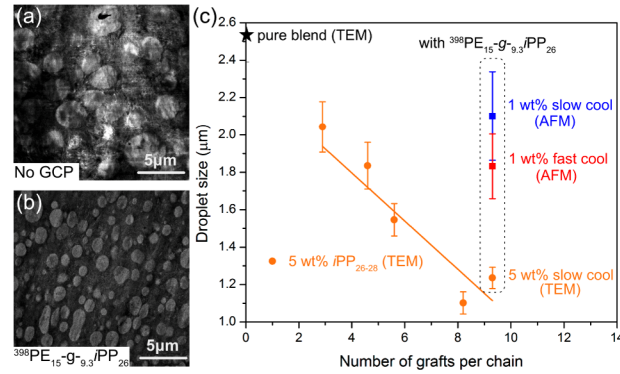


Figure 1. TEM images and *i*PP average droplet size of *i*PP/HDPE 30/70 blends with (a) no compatibilizer and (b) 5 wt % $^{398}PE_{15-g-9.3}iPP_{26}$ compatibilizer. (c) Effect of number of grafts/chain on droplet size for 5 wt % (orange; 10 K/min cooling rate) and 1 wt % (blue and red at 10 and 23 K/min cooling rates, respectively) $^{398}PE_{15-g-9.3}iPP_{26}$ compatibilizer. The error bars are 95% confidence intervals.

phase appears as brighter islands in the HDPE matrix. For a given graft length, samples with a larger number of grafts per chain exhibit smaller dispersed phases (Figure 1c). For the blend containing 5 wt % iPP_{26-28} GCP, the average *i*PP domain diameter decreased from 2.5 to 1.2 μ m as the average number of grafts/chain increased from 0 to 9 grafts/chain. Similar results were observed for the iPP_{14} and iPP_6 grafts (Figure S7). For comparison to 5 wt % GCP, the *i*PP droplet size of blend samples containing 1 wt % $^{398}PE_{15-g-9.3}iPP_{26}$ GCP were analyzed by atomic force microscopy (AFM; Figure S6). The average droplet size was about 2 μ m, with a slightly smaller average droplet size observed when the sample was cooled at 23 K/min versus 10 K/min (vide infra) after melt pressing, possibly due to additional domain coarsening during the slow cooling. All these results show that properly designed GCPs drive reductions in the dispersed phase droplet size, presumably by localizing at the interface and reducing the interfacial tension of the *i*PP/HDPE blends in a manner typical of a good compatibilizer.

Individually, the *i*PP and HDPE homopolymer samples employed in this study display ductile behavior (i.e., >600% strain at break), with strain hardening at larger elongations (Figure S8, panels A1–D1). However, when these polymers are melt-blended (*i*PP/HDPE = 30/70 w/w) without compatibilizer, the resulting mixture shows a dramatic reduction in ductility (i.e., <20% strain at break) compared to the neat materials (Figure S8, panels Z and E1).^{15,16} Ideally, the tensile behavior (i.e., elongation and toughness) of compatibilized blends should be intermediate to that of the HDPE and *i*PP homopolymers, a feature that would be indicative of a good compatibilizer. To test the effectiveness of the GCPs, the mechanical properties of *i*PP/HDPE blends were first evaluated with 5 wt % GCP (Figures 2a and S8); this

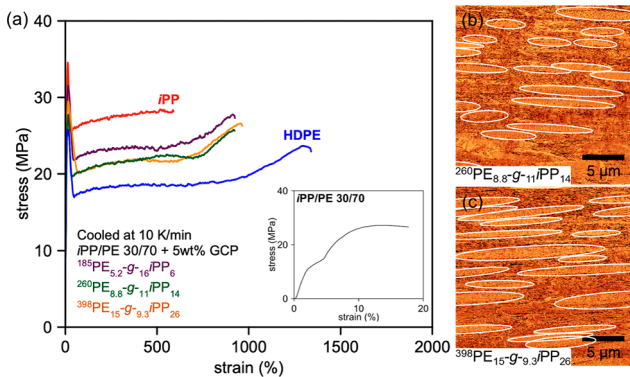


Figure 2. (a) Representative uniaxial tensile elongation experiments of pure HDPE and iPP and blends of 30/70 iPP/HDPE with PE-g-iPP copolymers of varied graft size (5 wt % of GCP cooled at 10 K/min). (b, c) Representative AFM images of stretched tensile test samples blended with GCPs of varied graft size; ellipses are added for visualization of elongated droplets. See Figure S9 for raw data.

relatively high GCP loading was selected to probe the effect of the graft length and density. For all three graft lengths, improved elongation was achieved in blends compatibilized with graft copolymers containing a larger number of grafts (Figure 2a). As an example, for the GCP's containing the 6 kDa iPP grafts, the strain at break increased from 100% to 950% in strain at break when the average number of grafts per chain was raised from 10 (Figure S8, panel B) to 16 (Figures 2a and S8, panel A). For two of the samples in Figure 2a, it is noteworthy that AFM images (Figures 2b,c and S9) of cross sections near (i.e., within 1 cm) the fracture surface showed that the iPP droplets deformed into highly extended ellipsoids elongated in the tensile direction. Qualitatively, it appears that the droplets deformed in a manner commensurate with the deformation of the HDPE matrix. Importantly, there were no detectable voids indicative of cavitation at the interface between the deformed iPP droplets and the HDPE matrix. Void formation upon straining the 30/70 iPP/PE blend was observed by SEM and is reported in our previous study.¹⁵ This suggests the GCPs localize at the interface and facilitate strong interfacial adhesion that can aid in stress transfer between the two phases; this observation is consistent with the toughness and high elongation of these compatibilized blends. Notably, PE-g-iPP additives do not produce as much iPP microdomain size reduction as PE-*b*-iPP or PE-g-*a*PP containing blends.^{15,16,21} Apparently, the graft-block molecular architecture is less efficient at saturating the particle–matrix interface and reducing interfacial tension and the average particle size. Nevertheless, there is sufficient interfacial coverage to inhibit cavitation during tensile tests.

We also evaluated the effect of graft length on tensile properties (Figure 3). As the molecular weight of the grafts increased from 6 to 26 kDa, the higher molecular weight macromonomer variants required fewer grafts to achieve improved toughness. Similar tensile properties were obtained with 16 grafts per chain of 6 kDa grafts (Table 1, entry 1) and 11 grafts per chain of 14 kDa grafts (Table 1, entry 6); for the 26 kDa grafts, high strain at break was observed for as few as an average of 5.6 grafts/chain (Table 1, entry 11).

Having established the effect of the graft number and length, we investigated the mechanical compatibilization efficiency at lower loadings of graft copolymer. Under the base cooling conditions (10 K/min), blends containing 1 wt % GCP

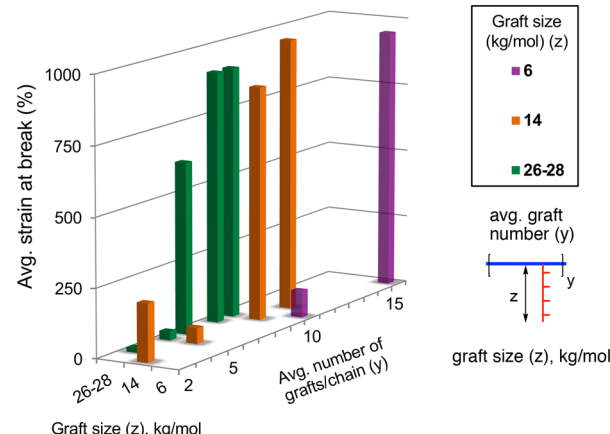


Figure 3. Average strain at break for blends of 30/70 iPP/HDPE containing 5 wt % PE-g-iPP copolymers cooled at 10 K/min. A minimum of five tensile measurements were performed for each blend. Graft copolymers containing 26k and 28k grafts are shown in the same series. See Table 1 for standard deviation.

showed lower strain at break compared to the 5 wt % samples prepared with the same cooling rate (10 K/min, Figure 4a). We hypothesize that, at the lower GCP loading, there is less interfacial coverage of the GCP and therefore reduced ability to transfer stress across the interface.

We also investigated the effect of cooling rate on the tensile properties of the melt pressed samples. At 1 wt % GCP loading, faster cooling (23 K/min) yielded samples with improved toughness relative to those cooled more slowly (10 K/min; Figures 4b and S8). At 1 wt % $^{260}\text{PE}_{8.8}g_{11}\text{iPP}_{14}$ loading, the samples showed a strain at break of 800% compared to 250% at the slower cooling rate for the same additive. This is an anticipated result, as slow cooling yields polymers with higher crystallinity and more brittle behavior, which is evident in the stress–strain curves for the pure iPP and HDPE (Figure 4). For all the samples, with and without GCP, the modulus values (stress) between about 20% and 500–800% strain for the faster cooling rate (Figure 4b) are about 15% lower than observed at the slower cooling rate (Figure 4a). This likely reflects lower crystallinity at the faster cooling rate. iPP and HDPE homopolymers showed higher strain at break and more strain hardening when cooled at 23 K/min than at 10 K/min, also consistent with a higher rubbery amorphous content. However, the 30/70 iPP/HDPE blend showed similar, brittle, tensile behavior at both cooling rates (insets in Figure 4). The overall toughness of the best GCP containing blends is similar to that observed for blends containing linear PE-iPP tetra- and hexablock copolymers.^{15,16}

DSC analysis of the graft copolymers (Figure S3) shows an endotherm associated with residual macromonomer, which may cocrystallize with iPP grafts and a second endotherm that corresponds to PE. At a higher number of grafts/chain, a third endotherm due to the backbone is observed, with a peak temperature similar to that of LLDPE. This shows that the backbone and graft chains independently crystallize. Similar crystallization with the homopolymers will inhibit interfacial delamination, resulting in toughness. This will be operative in the slow and fast cooled mixtures.

The results from the tensile tests and TEM and AFM studies demonstrate that the PE-g-iPP copolymer additives act as good compatibilizers for iPP/HDPE blends. In general, increasing the number of grafts and increasing the graft length increases

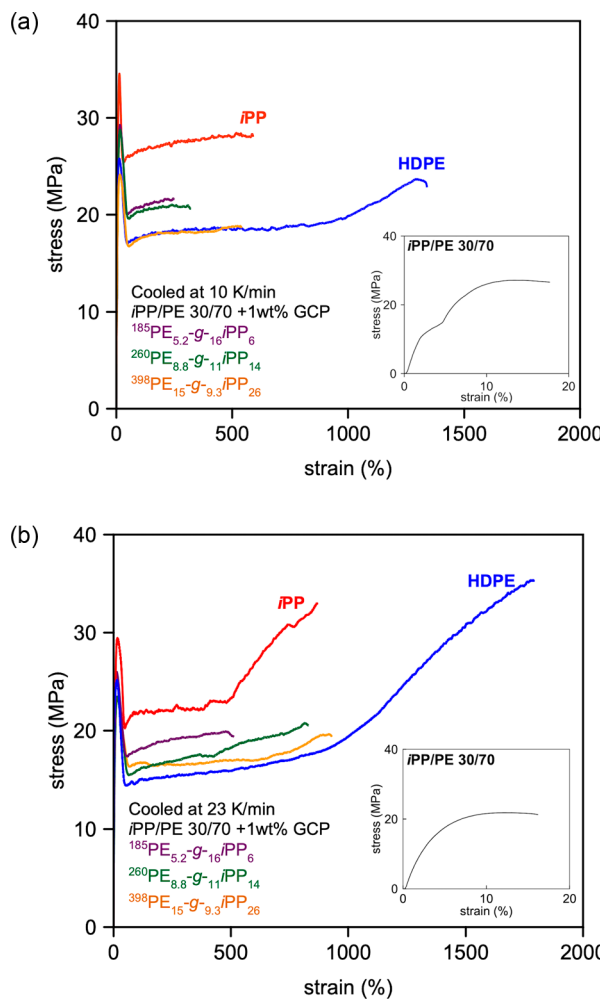


Figure 4. Representative uniaxial tensile elongation experiments of pure HDPE and iPP and blends of 30/70 iPP/HDPE with PE-g-iPP copolymers of varied graft size with 1 wt % of GCP (a) cooled at 10 K/min and (b) cooled at 23 K/min.

the tensile strength of compatibilized blends. As a comparison, the tensile strength for the rapidly cooled 1 wt % GCP containing blends is roughly comparable to that observed for well-defined PE-iPP tetra- and hexablocks.^{15,16} These findings suggest that efficient compatibilizers for HDPE and iPP may be prepared by nonliving polymerization routes and may ultimately provide more economical syntheses of these useful materials. We are currently investigating the mechanism of compatibilization for the graft copolymers and exploring other polymer architectures.

■ ASSOCIATED CONTENT

si Supporting Information

The Supporting Information is available free of charge at <https://pubs.acs.org/doi/10.1021/acsmacrolett.0c00339>.

Complete descriptions of experimental procedures, including macromonomer and polymer syntheses, GPC traces, tensile elongation traces, AFM, TEM imaging, and DSC curves (PDF)

■ AUTHOR INFORMATION

Corresponding Authors

Christopher J. Ellison — Department of Chemical Engineering and Materials Science, University of Minnesota, Minneapolis, Minnesota 55455, United States; orcid.org/0000-0002-0393-2941; Email: cellison@umn.edu

Anne M. LaPointe — Department of Chemistry and Chemical Biology, Baker Laboratory, Cornell University, Ithaca, New York 14853, United States; orcid.org/0000-0002-7830-0922; Email: lapointe@cornell.edu

Frank S. Bates — Department of Chemical Engineering and Materials Science, University of Minnesota, Minneapolis, Minnesota 55455, United States; orcid.org/0000-0003-3977-1278; Email: bates001@umn.edu

Geoffrey W. Coates — Department of Chemistry and Chemical Biology, Baker Laboratory, Cornell University, Ithaca, New York 14853, United States; orcid.org/0000-0002-3400-2552; Email: coates@cornell.edu

Authors

Kristine Klimovica — Department of Chemistry and Chemical Biology, Baker Laboratory, Cornell University, Ithaca, New York 14853, United States

Sanshui Pan — Department of Chemical Engineering and Materials Science, University of Minnesota, Minneapolis, Minnesota 55455, United States

Ting-Wei Lin — Department of Chemistry and Chemical Biology, Baker Laboratory, Cornell University, Ithaca, New York 14853, United States

Xiayu Peng — Department of Chemical Engineering and Materials Science, University of Minnesota, Minneapolis, Minnesota 55455, United States; orcid.org/0000-0002-6216-7493

Complete contact information is available at: <https://pubs.acs.org/10.1021/acsmacrolett.0c00339>

Author Contributions

The manuscript was written through contributions of all authors. All authors have given approval to the final version of the manuscript.

Funding

This work was supported by the NSF Center for Sustainable Polymers (CHE-1901635). This work made use of the NMR Facility at Cornell University and is supported, in part, by the NSF under Award CHE-1531632. Some of the experiments were conducted in the Characterization Facility, University of Minnesota, which receives partial support from NSF through the MRSEC program.

Notes

The authors declare no competing financial interest.

■ REFERENCES

- (1) Geyer, R.; Jambeck, J. R.; Law, K. L. Production, use, and fate of all plastics ever made. *Sci. Adv.* **2017**, *3*, No. e1700782.
- (2) *Chemical and Engineering News* **2018**, Vol. 96, Issue 25, pp 26–29.
- (3) Graziano, A.; Jaffer, S.; Sain, M. Review on modification strategies of polyethylene/polypropylene immiscible thermoplastic polymer blends for enhancing their mechanical behavior. *J. Elastomers Plast.* **2019**, *51*, 291–336.
- (4) Chaffin, K. A.; Knutson, J. S.; Brant, P.; Bates, F. S. High-Strength Welds in Metallocene Polypropylene/Polyethylene Laminates. *Science* **2000**, *288*, 2187–2190.

(5) Stehling, F. C.; Huff, T.; Speed, C. S.; Wissler, G. Structure and Properties of Rubber-Modified Polypropylene Impact Blends. *J. Appl. Polym. Sci.* **1981**, *26*, 2693–2711.

(6) D’Orazio, L.; Greco, R.; Martuscelli, E.; Ragosta, G. Effect of the Addition of EPM Copolymers on the Properties of High Density Polyethylene/Isotactic Polypropylene Blends: II. Morphology and Mechanical Properties of Extruded Samples. *Polym. Eng. Sci.* **1983**, *23*, 489–497.

(7) Anastasiadis, S. H.; Gancarz, I.; Koberstein, J. T. Compatibilizing Effect of Block Copolymers Added to the Polymer/Polymer Interface. *Macromolecules* **1989**, *22*, 1449–1453.

(8) Bucknall, D. G.; Higgins, J. S.; Rostami, S. The compatibilizing effect of diblock copolymer on the morphology of immiscible polymer blends. *Polymer* **1992**, *33*, 4419–4422.

(9) Macosko, C. W.; Guégan, P.; Khandpur, A. K.; Nakayama, A.; Marechal, P.; Inoue, T. Compatibilizers for Melt Blending: Premade Block Copolymers. *Macromolecules* **1996**, *29*, 5590–5598.

(10) Arriola, D. J.; Carnahan, E. M.; Hustad, P. D.; Kuhlman, R. L.; Wenzel, T. T. Catalytic Production of Olefin Block Copolymers Via Chain Shuttling Polymerization. *Science* **2006**, *312*, 714–719.

(11) Lin, Y.; Marchand, G. R.; Hiltner, A.; Baer, E. Adhesion of Olefin Block Copolymers to Polypropylene and High Density Polyethylene and Their Effectiveness as Compatibilizers in Blends. *Polymer* **2011**, *52*, 1635–1644.

(12) Lin, Y.; Yakovleva, V.; Chen, H.; Hiltner, A.; Baer, E. Comparison of Olefin Copolymers as Compatibilizers for Polypropylene and High-Density Polyethylene. *J. Appl. Polym. Sci.* **2009**, *113*, 1945–1952.

(13) Shan, C. L. P.; Walton, K. L.; Marchand, G. R.; Carnahan, E. M.; Karjala, T. Crystalline block composites as compatibilizers. U.S. Patent 8,822,599, 2014.

(14) Hu, Y.; Conley, B.; Walton, K. L.; Collin, L. P. S.; Marchand, G. R.; Patel, R. M.; Kupsch, E.-M.; Walther, B. W. Multilayered Polyolefin-Based Films. U.S. Patent 9,511,567, 2016.

(15) Eagan, J. M.; Xu, J.; Di Girolamo, R.; Thurber, C. M.; Macosko, C. W.; LaPointe, A. M.; Bates, F. S.; Coates, G. W. Combining Polyethylene and Polypropylene: Enhanced Performance with PE/iPP Multiblock Polymers. *Science* **2017**, *355*, 814–816.

(16) Xu, J.; Eagan, J. M.; Kim, S.-S.; Pan, S.; Lee, B.; Klimovica, K.; Jin, K.; Lin, T.-W.; Howard, M. J.; Ellison, C. J.; LaPointe, A. M.; Coates, G. W.; Bates, F. S. Compatibilization of Isotactic Polypropylene (iPP) and High-Density Polyethylene (HDPE) with iPP–PE Multiblock Copolymers. *Macromolecules* **2018**, *51*, 8585–8563.

(17) Ohtaki, H.; Deplace, F.; Vo, G. D.; LaPointe, A. M.; Shimizu, F.; Sugano, T.; Kramer, E. J.; Fredrickson, G. H.; Coates, G. W. Allyl-Terminated Polypropylene Macromonomers: A Route to Polyolefin Elastomers with Excellent Elastic Behavior. *Macromolecules* **2015**, *48*, 7489–7494.

(18) Liu, W.; Liu, P.; Wang, W.-J.; Li, B. G.; Zhu, S. A Comprehensive Review on Controlled Synthesis of Long-Chain-Branched Polyolefins: Part 2, Multiple Catalyst Systems and Prepolymer Modification. *Macromol. React. Eng.* **2016**, *10*, 180–200.

(19) Kashiwa, N.; Kojo, S.-I.; Kawahara, N.; Matsuo, S.; Kaneko, H.; Matsugi, T. New methodology for synthesizing polyolefinic graft block copolymers and their morphological features. *Macromol. Symp.* **2003**, *201*, 319–326.

(20) Tsou, A. H.; López-Barrón, C. R.; Jiang, P.; Crowther, D. J.; Zeng, Y. Bimodal Poly(Ethylene-cb-Propylene) Comb Block Copolymers from Serial Reactors: Synthesis and Applications as Processability Additives and Blend Compatibilizers. *Polymer* **2016**, *104*, 72–82.

(21) López-Barrón, C. R.; Tsou, A. H. Strain Hardening of Polyethylene/Polypropylene Blends Via Interfacial Reinforcement with Poly(Ethylene-cb-Propylene) Comb Block Copolymers. *Macromolecules* **2017**, *50*, 2986–2995.

(22) Stockland, R. A.; Foley, S. R.; Jordan, R. F. Reaction of Vinyl Chloride with Group 4 Metal Olefin Polymerization Catalysts. *J. Am. Chem. Soc.* **2003**, *125*, 796–809.

(23) Gaynor, S. G. Vinyl Chloride as a Chain Transfer Agent in Olefin Polymerizations: Preparation of Highly Branched and End Functional Polyolefins. *Macromolecules* **2003**, *36*, 4692–4698.

(24) During the synthesis of PE-iPP multiblock copolymers, we observed that the polymerization continues even after polymer precipitation occurs, suggesting that the gaseous monomer can diffuse into the swollen polymer matrix. Under these conditions, however, macromonomer insertion is predicted to be strongly disfavored.

(25) Brown, G. M.; Butler, J. H. New Method for the Characterization of Domain Morphology of Polymer Blends Using Ruthenium Tetroxide Staining and Low Voltage Scanning Electron Microscopy (LVSEM). *Polymer* **1997**, *38*, 3937–3945.